Measurement of the bubble population in coastal waters using combination frequencies of MHz order

Timothy G. Leighton, Andy D. Phelps and David G. Ramble

Institute of Sound and Vibration Research,
University of Southampton,
Highfield, Southampton, UK
Email: tgl@isvr.soton.ac.uk

Abstract

This paper describes the use of a combination frequency technique to measure the size distribution of oceanic bubbles. Written between two sea trials, the paper describes how the apparatus can be adapted to design tests for specific environments and data requirements. Parameters which can be changed are the sensing volume, the bubble radii for which data points are taken, and the degree of time resolution in the bubble counts.

1. Introduction

The ability to size and count gas bubbles in liquid has many applications relevant to ocean science, including studies into ambient noise [1,2], the near-surface acoustic waveguide [3,4], the atmosphere/ocean fluxes of mass, momentum and energy [5,6], precipitation [7,8], diver safety [9-11], dynamic loading on structures, sonar occlusion, cavitation inception [12], and passive sensing [13]. Because of the differing compressibilities of the gas and liquid, and the impedance mismatch at the bubble wall, acoustic techniques for bubble detection can be effective. Notably, measurement of the resonance frequency ν_r of a bubble can be used to estimate its equilibrium radius R_0, since ν_r is approximately inversely proportional to the bubble radius [14] (e.g. $\nu_r R_0 \approx 0.01 \sqrt{p_0}$ for air bubbles of $R_0 >\sim 10$ μm in water of static pressure p_0).

A sound field of given angular frequency ω_p (here termed the 'pumping' frequency) can drive a bubble into nonlinear oscillation such that it backscatters a range of frequencies including ω_p, $2\omega_p$, $3\omega_p$ ..., $\omega_p/2$, $3\omega_p/2$ ... etc. The closer ω_p is to the bubble resonance, the stronger in general these emissions. Although bubble sizing has been attempted using these signals, as well as with Doppler techniques and geometrical imaging, all such signals possess limitations [15]: the detector may, for example, mistake a cluster of small bubbles, or a single large bubble, for a resonant bubble. In the method used in this paper the bubble is insonated by the 'pump' frequency ω_p *plus* a higher, fixed, 'imaging' frequency ω_i. Because the latter is much higher than ω_p, the bubble pulsation is effectively 'frozen' during a single imaging cycle. Thus the returned signal is a measure of the geometric scattering from a target whose acoustic cross-section varies periodically. This is shown in figure 1, where the signal returned by the bubble consists of the imaging frequency, amplitude modulated by the pump frequency. Consequently the spectrum of the returned signal contains peaks at $\omega_i \pm \omega_p$, the amplitudes of which increase with the pulsation amplitude of the bubble and therefore, if the amplitude of the pump signal is frequency-independent, with the nearness of ω_p to the bubble resonance. If the off-resonance contributions from bubbles of a size similar to those resonant at ω_p can be incorporated into an analysis of the $\omega_i \pm \omega_p$ signals, then in principle the $\omega_i \pm \omega_p$ signals can be used to estimate the number of bubbles resonant at ω_p in the sensing volume. The two-frequency insonation may also generate signals at $\omega_i \pm \omega_p/2$ with much reduced off-resonance and non-bubble contributions than the $\omega_i \pm \omega_p$ signal [16]. In both techniques the high frequencies allow specific spatial localisation, and low signal-to-noise ratios since bubble-mediated information is transposed from a comparatively noisy frequency window around ω_p up to a frequency window around ω_i. Whilst $\omega_i \pm \omega_p/2$ signals are appropriate for high-accuracy measurements of individual bubbles (as might be useful as a sensor for pressure changes [17]), the parametric nature of the emissions require that the pump signal amplitude at the bubble must be very well controlled. This makes it less suitable for bubble measurement in the oceanic environment than the $\omega_i \pm \omega_p$ signal used here. When the $\omega_i \pm \omega_p$ technique is used at sea,

care must be taken to account correctly for the contributions to the signal of off-resonant, and non-bubble, sources, and the techniques for so doing are now described.

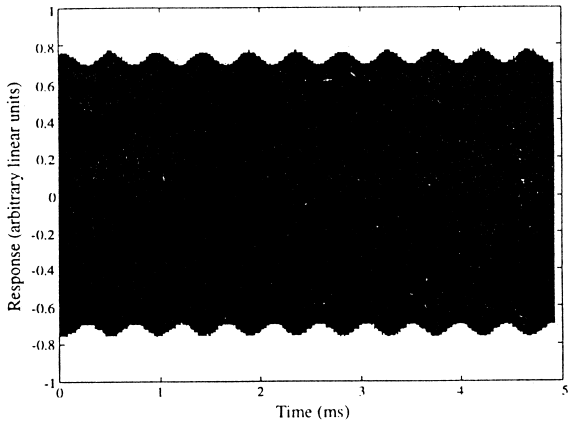

Figure 1. *Returned signals from a bubble insonated at two frequencies, measured with a high frequency probe - the high frequency imaging signal was set at 1.1 MHz, and the bubble resonance/pump frequency at 2160 Hz. The data was sampled at 10 MHz on a LeCroy 9314L digital oscilloscope. The pump signal amplitude is 25 Pa. The high carrier frequency plots so densely as to appear black in the figure.*

Earlier workers investigated the $\omega_i \pm \omega_p$ signal for measuring an oceanic bubble population [18], using a chirped signal between 2.5 and 6 kHz, with an imaging frequency of 450 kHz. However in those tests no distinction was made between bubble-mediated coupling and that caused by turbulence, and no compensation was made either for the significant off-resonance nature of the $\omega_i \pm \omega_p$ signal, or for the pump transducer frequency response. Later workers documented how turbulent effects can be distinguished from the bubble signals, and compensation made for the off-resonant contribution to the $\omega_i \pm \omega_p$ signal [19]. By employing discrete tones as the pump signal, the variable frequency response of the source transducer could be removed allowing constant and clearly-defined bubble insonation conditions. Interpretation of the energy at the $\omega_i \pm \omega_p$ frequencies in terms of bubble numbers requires modelling of the bubble response. The method used here produces absolute bubble counts, rather than relying on adjustable parameters or fitting models based on historical measurements to the data. Both current and earlier workers [18-21] used simplified forms of the Rayleigh-Plesset equation, which are used to obtain expressions for the pressure amplitudes at the various frequency locations [20,21]. However these earlier procedures [18,20,21] took account only of viscous damping of the bubble motion, which for the bubbles under discussion here and earlier is an order of magnitude smaller than damping through thermal and radiation losses (Newhouse and Shankar [21] made the damping an unknown variable which they optimised to give best fit between their measured data and the bubble counts they expected). Ignoring the thermal and radiation effects produces errors of > 36 dB in relative energies invested at ω_i and $\omega_i \pm \omega_p$. The algorithm for interpreting acoustic data in terms of bubble counts used in this paper incorporates all three damping mechanisms, and reduces such errors to < 1 dB. Full details of the analysis, and of its use in the calibration of the bubble detector (which will be summarised in section 2.1) have been reported elsewhere [19].

2. Materials and methods

2.1 Laboratory calibration

Calibration of the apparatus was performed to ensure that the energy of the $\omega_i \pm \omega_p$ signals could be related to the signal strength associated with one resonant bubble. This was achieved through examination of the acoustic scattering from a steady stream of bubbles of known size. The equipment schematic is shown in figure 2. The pump frequency signal was generated using a Tektronix 2005 arbitrary waveform generator controlled via a GPIB cable connected to a PC, which was passed into a Bruel and Kjaer 2713A power amplifier. The pump transducer comprised a 104 mm inside diameter piezoceramic ring transducer which was set into a polyurethane foam and encased in a nylon housing. The imaging signal was generated by a 1 MHz crystal oscillator amplified with an ENI 240L RF power amplifier, and this was passed to the imaging signal transducer (the head of a Therasonic 1030 ultrasonic therapy unit as manufactured by Electro Medical Supplies) which was potted inside a 45 mm diameter

aluminium cylinder to protect it when used in the open sea. The imaging signal amplitude at the focus of the two transducers was measured as 30 kPa using a calibrated needle hydrophone (active element diameter = 0.5 mm) with a HP1 submersible pre-amplifier, as manufactured by Precision Acoustics Ltd.

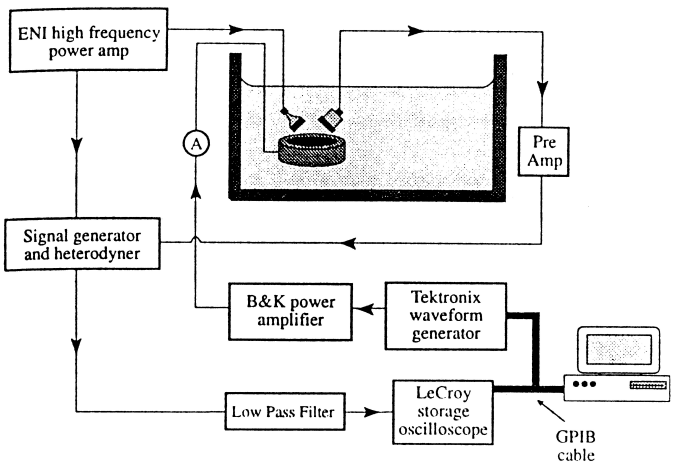

Figure 2. Schematic of the equipment used in the lab tests

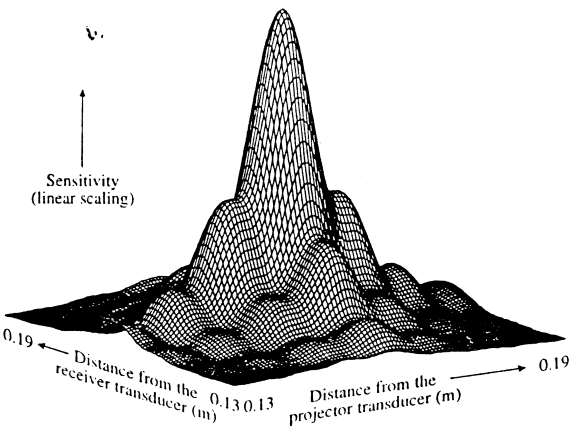

Figure 3. The sensitivity within the sampling volume, for the geometry employed in the Channel test.

The returned signal from the bubble was monitored using a Panametrics V302 piezoceramic transducer, similarly potted in a 45 mm diameter sleeve, and conditioned using a Panametrics 5670 preamplifier. The preamplified signal was then heterodyned with a reference signal from the crystal oscillator: this results in the useful information contained just above and below the imaging frequency being reproduced at just above dc, enabling much lower sampling rates and data storage. The low frequency information was filtered to prevent aliasing using a Barr and Stroud EF5-02 46 dB/octave filter and acquired by a LeCroy 9314L storage oscilloscope. For the laboratory tests the data was sampled at 50 kHz and 10,000 points taken.

Calibration involved, first, verification of the model through comparison of its predictions with the measured energy distribution in the spectra scattered from the bubbles in the stream. Second, the sensitivity of the high frequency receiver transducer was estimated. Third, the behaviour of resonant bubbles at the specific pump frequencies used in the oceanic tests were modelled (using parameters applicable to sea water, rather than those of fresh water as used in modelling the lab tests). With application of the same sensitivity adjustment and the relevant preamplifier / heterodyner corrections, this provided an estimate of the signal levels expected from the different bubbles resonant at the specific pump frequencies chosen.

The calibration was done once in November 1995 in preparation for tests in the surf zone off a beach in the North Sea, and again in March 1997 before tests in deeper water in the English Channel. In each case the transducer geometry employed in the tank tests was unchanged for the subsequent ocean trial, which allowed certain parameters in the pulsation model to be poorly defined without any loss of accuracy [19]. However the two ocean tests used different transducer geometries, so that the sampling volume of the instrument was smaller for the North Sea trial (0.2 cm^3) than in the English Channel trial (1.0 cm^3). This change was made because in the first test a very small test volume was desirable since it was supposed that the bubble number densities would be very high, so that reducing the volume would reduce the chance of acoustic shielding causing under-counting. It was also of interest to investigate how small a test volume could reasonably be generated with this apparatus. However for the English Channel tests, a larger test volume was desirable (to lessen the effect of spatial inhomogeneity in the bubble field by sampling a larger volume) and allowable (since predictions suggested that the bubble densities would be lower out of the surf zone). In each case the sensing volume was calculated by modelling the beam patterns of the two high frequency transducers using a Rayleigh integral over their surfaces. When these patterns were overlapped in the same layout as the transducer arrangement, they allowed the insonation volume to be estimated. This gave an insonation volume, defined by where the sensitivity fell off to 3 dB of its peak value. The result of such a procedure for the English Channel transducer geometry is shown in figure 3, where the distance between both the high frequency transducers and the focus is 16 cm.

2.2 Oceanic data collection

The equipment used in the sea trials was largely similar to that used in the laboratory experiments, and the schematic is shown in figure 4. The most important difference in the layout of the oceanic equipment is the provision of a remote equipment canister, which was set up in the sea and attached to the land based equipment via an underwater bulkhead connector and 200 m of waterproof cable, as manufactured by PDM Group. The canister comprised a 1000 mm long × 355 mm diameter watertight aluminium alloy cylinder, which was painted to minimise corrosion, and clamped to a rigid scaffold structure as shown in figure 5. This canister contained the high frequency power amplifier, the crystal oscillator and heterodyner equipment, the returned signal RF preamplifier, and a temperature sensor to monitor the effects that the enclosed space had on the potential of the equipment to overheat. Additionally, a differential amplifier pair was added to the returned signal circuit to ensure that no signal corruption occurred when passed down the 200 m cable: this additional step was analysed in the laboratory and its frequency response quantified. Because of the higher pump frequencies involved, the data was sampled at 500 kHz, and 50,000 points were taken. To speed up the data collection and storage, the Tektronix output waveform comprised all four frequencies in one signal, and the LeCroy oscilloscope sampling the data was triggered by markers from the signal generator to allow the individual sections to be identified in the returned waveform.

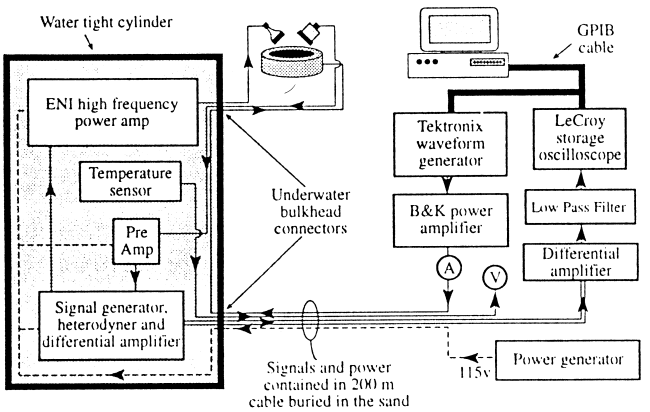

Figure 4. Schematic of the apparatus

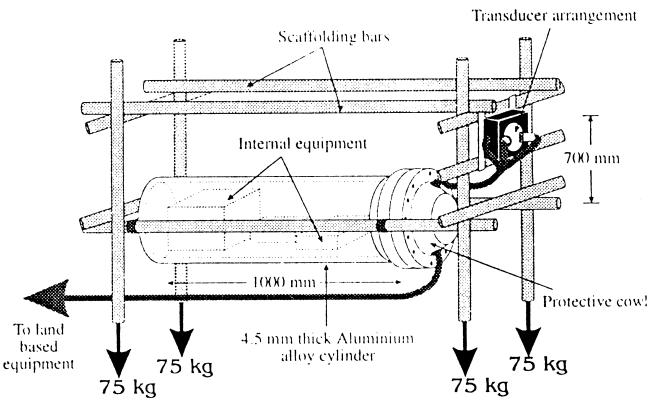

Figure 5. The arrangement of the cylinder for the North Sea test

Preliminary calibration tests were carried out to ensure that the pump signal amplitude was constant for all the pump frequencies employed in a given test. The transducer head was immersed in a test tank to the same depth that it would have whilst activated in the oceanic tests. Then the pump signal amplitude measured with a constant input signal level at each of the pump frequencies using a Bruel and Kjaer 8103 hydrophone conditioned with an 2635 charge amplifier. This allowed the frequency response of the pump transducer to be inverted, and a constant and known pump signal amplitude to be employed.

The specific pump frequencies chosen for the North Sea tests were 28, 50, 60 and 88 kHz, so that three of these would coincide with measurements made in an earlier bubble count using the resonant backscatter from bubbles [4]. This paper is written just prior to the Channel test, for which the rig will employ two different pump signal regimes. In the first, pump frequencies of 17, 28, 50, 60, 88, 10, 145, 165, 180 and 200 kHz will be used, corresponding to bubble radii of 200, 120, 66, 55, 37, 30, 23, 20, 18 and 16 μm. These were chosen since examination of earlier test results [4] indicated that, with bubble radius plotted on a logarithmic scale as is usual, these points would readily identify a possible peak in the spectrum at around $R \sim 20$ μm [4], whilst also indicating key gradients in the curve. The second regime will use fewer pump frequencies, enabling finer time resolution: the interval between consecutive tests using the 10 pump frequencies in the first regime is 3 s, whilst in the second, where only 2 pump frequencies (17 and 145 kHz) are used, it is reduced to 0.85 s. Table 1 summarises the key parameters in the oceanic tests, showing how the same apparatus can be adapted to change the parameters of the investigation, giving the experimenter flexibility to design a given test to meet a specific requirement.

The North Sea tests occurred between 26th and 30th November 1995, on a beach in Tunstall, East Yorkshire, and were carried out in tandem with a group from the Southampton Oceanography Centre. Data was taken over a 3.5 minute period every half hour while the transducers were immersed. As the signals were broadcast consecutively with no gap, each measurement lasted only 0.4 s. The beach was chosen because of its slight gradient, which allowed the equipment to be set up at low tide and anchored to the beach, such that as the tide

came in it would eventually cover the rig to enable measurements to be taken. The rig was weighed down with 75 kg metal weights at each corner which were buried in the sand.

Parameter	North Sea test	Channel test (regime 1)	Channel test (regime 2)
Pump frequencies (kHz)	28, 50, 60, 88	17, 28, 50, 60, 88, 110, 145, 165, 180, 200	17, 145
Pump amplitude at bubble (Pa)	3000	3000	3000
Sensing volume (cm^3)	0.2	1.0	1.0
Depth of sensor (m)	1.5	0.8	0.8
Time per pump frequency (ms)	100	20	20
Interval between repeats (s)	9	3	0.85

Table 1. *The key parameters of the apparatus for the North Sea test, and for the two Channel tests.*

3. Results

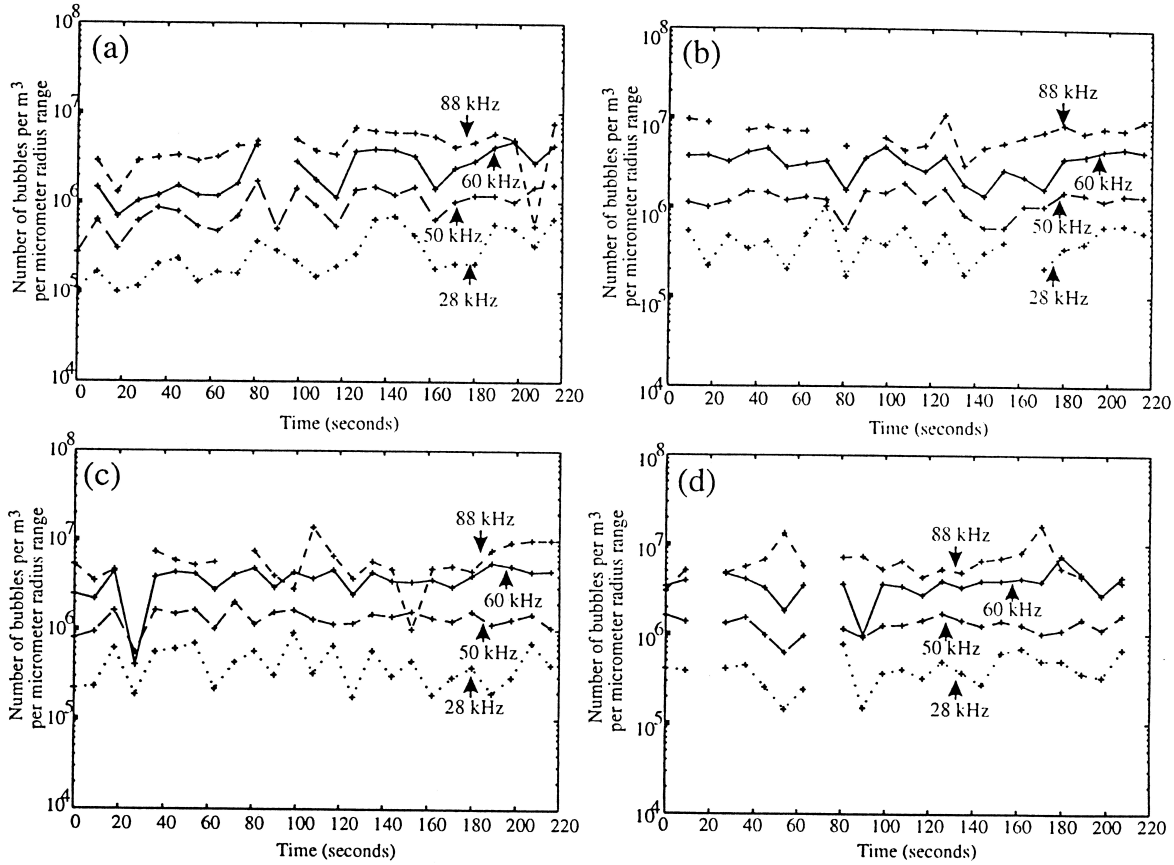

Figure 6. *The time-resolved bubble population densities, resonant at 28, 50, 60 and 88 kHz (i.e. of radius 120, 66, 55 and 37 μm respectively), measured at starting times of (a) 22.00, (b) 22.30, (c) 23.00 and (d) 23.30 GMT on 5 November 1995 in the surf zone at Tunstall. The error associated with each point is +200% and -50%. Some data points in the consecutive tests are missing. The bubble density is expressed in terms of the number of bubbles per cubic metre having a radius within a 1 μm range about the radius given.*

Figure 6 shows the time-resolved bubble counts found in the North Sea test. This degree of time-resolution is possible since the data is collected in a series of 0.4 s 'snap-shots', rather than requiring the time-averaging inherent in earlier studies. It should be noted that on occasions during the analysis the signal height dipped below the noise floor, and in these cases the particular readings have been left as gaps. In general, the smaller bubbles are the most

populous. Certain correlations between the counts of the various bubble sizes do appear at times (e.g. 120 - 180 s in (a); 20 - 40 s in (c)), although in the absence of other measurements there is no way of knowing the time-scales on which the population varies, and therefore whether any aliasing occurs. The time-average bubble counts, made by combining all the data in figure 6, have been reported in an earlier paper [19], in which the +200% and -50% error associated with each data point in figure 6, is described as arising primarily from the uncertainty associated with the sample volume: other sources of error are considered in that paper and found to be much less significant.

4. Discussion

In order to compare the time-resolved surf-zone data presented here with earlier historical measurements of the bubble population, the data must be time-averaged [19], and the results are given in figure 7. The graph suggests that, for a least-squares fit over the four points between 88 and 28 kHz (equivalent to $37 < R_0 < 120$ μm), the bubble distribution is fitted by $n(R_0) = aR_0^b$ where $n(R_0)$ is the number of bubbles per cubic metre having radii between R_0 and R_0+dR_0, and $a = 1.8 \times 10^{10}$ m^{-1} and $b = 2.3$, with associated errors for log (a / m) of ± 1.7 and for b of ± 0.9. This is higher than previous measurements, as would be expected in the surf zone. In deeper waters, the bubble population in the sea tends in the main to increase with wind speed and decrease with depth below the surface.

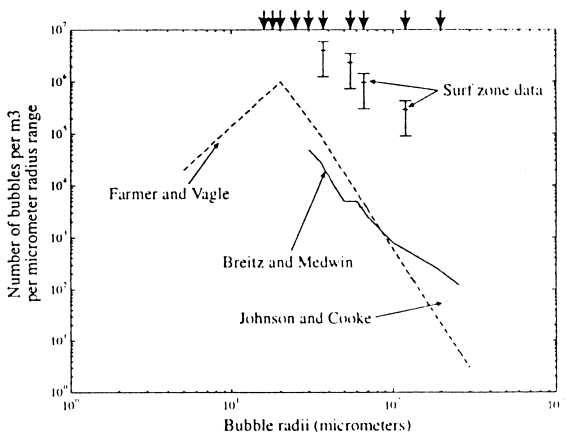

Figure 7: *Comparison of time-averaged data measured in the oceanic surf zone with historical estimates, taken from references [4], [24] and [30]. The error bars on the surf zone measurements mostly reflect an uncertainty in the measurement volume. The bubble population is expressed as the number of bubbles of a specific radius over a 1 μm range, per unit volume. The equilibrium radii corresponding to the frequencies anticipated in the Channel tests, regime 1, are also shown (arrowed).*

Optical investigations have indicated that most of the bubbles in the near-shore zone have equilibrium radii less than 100 μm [22]. Kolovayev [23] photographed and counted bubbles below breaking waves in the open sea at wind speeds of up to 13 m/s, by allowing them to rise onto a transparent plate. Dissolution may have occurred [6]. At depths between 1.5 and 8 m the most common bubbles were those possessing a radius of around 70 μm, and very few bubbles were larger than $R_0 \approx 300$ μm. Johnson and Cooke [24] photographed bubbles *in situ* in the sea, using a camera suspended from a surface float at depths of 0.5 to 4.0 m, and wind speeds of 8 to 13 m/s. They observed that the distribution of bubble size narrowed with increasing depth, the larger bubbles disappearing. The number of bubbles greater than the minimum size they could detect ($R_0 \approx 17$ μm) also decreased with increasing depth, decaying roughly exponentially over depth scales of order 1 m at wind speeds of 11 to 13 m/s, such that at a depth of 1.8 m the density of bubbles of a detectable size was 1.56×10^5 m^{-3}. They obtained a modal bubble radius in the size distribution of 40 - 50 μm. However Walsh and Mulhearn [25] suggest that the photographic observations lack the resolution to accurately count the smallest bubbles. MacIntyre [26] suggests that in addition to the lower limit imposed by resolution, there is an upper size limit on the reliable data resulting from poor statistics, so that only the data for bubbles in the range 60 μm $< R_0 <$ 150 μm is reliable. Medwin [27], making acoustic observations *in situ* through examination of attenuation at various frequencies, suggests that there is higher proportion of much smaller bubbles. Medwin and Breitz [28] confirm that the peak in the size spectrum occurs at a bubble radius less than 30 μm, and Su et al. [29] suggest that the peak is around 20 μm. Farmer and Vagle [4] deployed an upwardly-pointing four-frequency echo sounder (28, 50, 88 and 200 kHz) to investigate the bubble size distribution. Time-of-flight of reflected acoustic pulses gave a measure of distance, with a 10 cm

resolution for vertical samples. The backscattered intensities at the four frequencies for each vertical sample gave point measurements of the bubble population at four specific radii in the range $15 < R_0 < 100$ μm. These were then employed in an iterative calculation to give the size distribution of the whole population. They speculated that an upper bound on the size spectral peak occurs at $R_0 = 22$ μm, the true peak being closer to 20 μm.

Medwin and Breitz [28] have previously made measurements at depths less than 0.5 m, and they have used the variation in Q of several modes of a floating acoustical resonator to determine the bubble spectral size distribution at a depth of 0.25 m below a spilling oceanic breaker. The one-dimensional resonator consisted of a flat transducer facing a reflective plate 126 mm away, so that modes could be set up in the water between these. Bubbly water could flow in readily between the plates from the environment. From resonance broadening measurements for nine specific bubble sizes in the range 30 μm $< R_0 <$ 270 μm, Breitz and Medwin [30] found an average bubble density of $n(R_0) = 7.8 \times 10^8 \, (R_0 / \mu m)^{-2.7}$. In the same radius range the maximum bubble density detected was $n(R_0) = 1.6 \times 10^9 \, (R_0 / \mu m)^{-2.7}$. Both distributions agree with the Tunstall data, with respect to the value for the exponent b (within the ascribed error limits), but as expected the total population densities are higher in the surf zone measurements. Medwin and Breitz [28] however found that only the larger bubbles in the range 60 μm $< R_0 <$ 240 μm followed a $n(R_0) \propto (R_0 / \mu m)^{-2.6}$ distribution: the population of smaller bubbles (30 μm $< R_0 <$ 60 μm) decayed with depth as $n(R_0) \propto (R_0 / \mu m)^{-4}$. The size of the error bars associated with the Tunstall data prevent this kind of fine distinction. A $(R_0 / \mu m)^{-4}$ model distribution fits most of the data obtained by bubble counting reasonably well [5]. It was observations such as these that lead to the choice of frequencies employed in the Channel test. For the first regime, ten frequencies have been chosen (Table 1), corresponding to bubbles in the range 195 μm $> R_0 >$ 16 μm. The spacing of pump frequencies was chosen to allow resolution of the peak in the population density, which is expected to be at $R_0 \sim 20$ μm (figure 7). With ten pump frequencies, the temporal resolution is one sample every 3 s - this resolution is improved to a value of 0.85 s in the second test regime by restricting the number of pump frequencies to two (Table 1).

5. Conclusions

This paper described how a combination-frequency technique can be calibrated to give absolute bubble counts. Written after one trial and just prior to a second, it described how the apparatus could be adapted to allow the test to be designed to suit the environment and data requirements. Sensing volume, bubble radii investigated, and the degree of temporal resolution were all adjustable. For the surf zone measurements in the North Sea, a small sensing volume was required. The uncertainty associated with this volume was the main source of error in the final results. Four specific pump frequencies were investigated to enable comparison with historical data, and such a comparison is reported elsewhere [19]. Time-resolved data from such a test is presented here.

Acknowledgements

The authors wish to acknowledge the Natural Environment Research Council (grant GR3 09992) for support; and for assistance in the Tunstall trial, S.A. Thorpe, D. Baldwin, A. Hall, B. Stansbridge, D. Russell, J. Taylor, J. Hawkes, M. Bartlett and D. Edwards.

References

[1] G.M. Wenz, "Acoustic ambient noise in the ocean: spectra and sources," *J. Acoust. Soc. Am.*, vol. 34, pp. 1936-1956, 1962.

[2] M.S. Longuet-Higgins, "Bubble noise spectra," *J. Acoust. Soc. Am.*, vol. 87, pp. 652-661, 1990.

[3] M.J. Buckingham, "On acoustic transmission in ocean-surface waveguides," *Phil. Trans. R. Soc. Lond.*, vol. 335, pp. 513-555, 1991.

[4] D.M. Farmer and S. Vagle, "Waveguide propagation of ambient sound in the ocean-surface bubble layer," *J. Acoust. Soc. Am.*, vol. 86, pp. 1897-1908, 1989.

[5] D.K. Woolf and S.A. Thorpe, "Bubbles and the air-sea exchange of gases in near-saturation conditions," *J. Marine Res.*, vol. 49, pp. 435-466, 1991.

[6] S. Thorpe. "On the clouds of bubbles formed by breaking wind-waves in deep water, and their role in air-sea gas transfer," *Philos. Trans. R. Soc. London*, vol. A304, pp. 155-210, 1982.

[7] H.C. Pumphrey and P.A. Elmore, "The entrainment of bubbles by drop impacts," *J. Fluid Mech.*, vol. 220, pp. 539-548, 1990.

[8] J.A. Scrimger, D.J. Evans, G.A. McBean, D.M. Farmer and B.R. Kerman, "Underwater noise due to rain, hail and snow," *J. Acoust. Soc. Am.*, vol. 81, pp. 79-85, 1987.

[9] E.O. Belcher, "Quantification of bubbles formed in animals and man during decompression," *IEEE Trans. Biomed. Eng.*, vol. 27, pp. 330-338, 1980.

[10] T.G. Leighton, P.R. White and M.A. Marsden, "Applications of one-dimensional bubbles to lithotripsy, and to diver response to low frequency sound," *Acta Acustica*, vol. 3, pp. 517-529, 1995.

[11] L.A. Crum and Y. Mao, "Acoustically enhanced bubble growth at low frequencies and its implications for human diver and marine mammal safety," *J. Acoust. Soc. Am.*, Vol. 99, pp. 2898-2907, 1996.

[12] V.A. Akulichev, "Cavitation nuclei and thresholds of acoustic cavitation in ocean water," in *Bubble Dynamics and Interface Phenomena, Proceedings of an IUTAM Symposium (Birmingham, 6-9 Sept. 1993)*, edited by J.R. Blake, J.M. Boulton-Stone and N.H. Thomas, Kluwer Academic Publishers, The Netherlands, pp. 171-178, 1994.

[13] M.J. Buckingham and C.L. Epifanio, "Acoustic daylight imaging in the ocean: experimental results," in *3rd European Conference on Underwater Accoustics*, edited by J.S. Papadakis, Forth IACM, Crete, Greece, pp 341-347, 1996.

[14] T.G. Leighton, *The Acoustic Bubble*, Academic Press, London, 1994.

[15] T.G. Leighton, D.G. Ramble and A.D. Phelps, "The detection of tethered and rising bubbles using multiple acoustic techniques", *J. Acoust. Soc. Am.*, (in press).

[16] A.D. Phelps and T.G. Leighton, "High resolution bubble sizing through detection of the subharmonic response with a two frequency excitation technique", *J. Acoust. Soc. Am.*, vol. 99, pp. 1985-1992, 1996.

[17] E.G. Tickner, "Precision microbubbles for right side intercardiac pressure and flow measurements", In: *Contrast Echocardiography*, edited by R.S. Meltzer and J. Roeland, Nijhoff, London, 1982.

[18] D. Koller, Y. Li, P.M. Shankar and V.L. Newhouse, "High speed bubble sizing using the double frequency technique for oceanographic applications", *IEEE J. Oceanic Eng.*, vol. 17, pp. 288-291, 1992.

[19] A.D. Phelps, D.G. Ramble and T.G. Leighton, "The use of a combination frequency technique to measure the surf zone bubble population," *J. Acoust. Soc. Am.*, (in press).

[20] E.A. Zabolotskaya and S.I. Soluyan, "Emission of harmonic and combination-frequency waves by air bubbles", *Soviet Physics - Acoustics*, vol. 18, pp. 396-398, 1973.

[21] V.L. Newhouse and P.M. Shankar, "Bubble sizing using the nonlinear mixing of two frequencies", *J. Acoust. Soc. Am.*, vol. 75, pp. 1473-1477, 1984.

[22] D.C. Blanchard and A.H. Woodcock, "Bubble formation and modification in the sea and its meteorological significance," *Tellus*, vol. 9, pp. 145-158, 1957.

[23] P.A. Kolovayev, "Investigation of the concentration and statistical size distribution of wind produced bubbles in the near-surface ocean layer," *Oceanology*, vol. 15, pp. 659-661, 1976.

[24] B.D. Johnson and R.C. Cooke, "Bubble populations and spectra in coastal waters: a photographic approach," *J. Geophys. Res.*, vol. 84, C7, pp. 2761-3766, 1979.

[25] A.L. Walsh and P.J. Mulhearn, "Photographic measurements of bubble populations from breaking waves at sea," *J. Geophys. Res.*, vol. 92, pp. 14553-14656, 1987.

[26] F. MacIntyre, "On reconciling optical and acoustic bubble spectra in the mixed layer," In: *Oceanic whitecaps and their role in air-sea exchange processes*, edited by E.C. Monahan, I. O'Muircheartaigh and D. Reidel, Dordrecht, Holland, pp. 95-100, 1986.

[27] H. Medwin, "In situ acoustic measurements of microbubbles at sea," *J. Geophys. Res.*, vol. 82, pp. 971-976, 1977.

[28] H. Medwin and N.D. Breitz, "'Ambient and transient bubble spectral densities in quiescent seas and under spilling breakers," *J. Geophys. Res.*, vol. 94, pp. 12751-12759, 1989.

[29] M.Y. Su, S.C. Ling and J. Cartmill, "Optical measurements in the North Sea," In: *Sea surface sound*, edited by B. Kerman, Kluwer, Dordrecht, 1988.

[30] N. Breitz and H. Medwin, "Instrumentation for in situ acoustical measurements of bubble spectra under breaking waves,", *J. Acoust. Soc. Am.*, vol. 86, pp. 739-743, 1989.